Inorganic Chemistry

Article

pubs.acs.org/IC

Structural, Electronic, and Optical Features of $CuAl(S_{1-x}Se_x)_2$ Solar Cell Materials

M. G. Brik,*[,†,‡,§] M. Piasecki,[§] and I. V. Kityk[∥]

[†]College of Mathematics and Physics, Chongqing University of Posts and Telecommunications, Chongqing 400065, P. R. China

[‡]Institute of Physics, University of Tartu, Riia 142, Tartu 51014, Estonia

[§]Institute of Physics, Jan Dlugosz University, Armii Krajowej 13/15, PL-42200 Czestochowa, Poland

[∥]Institute of Materials Science and Engineering, Technical University of Czestochowa, Al. Armii Krajowej 19, PL-42200 Czestochowa, Poland

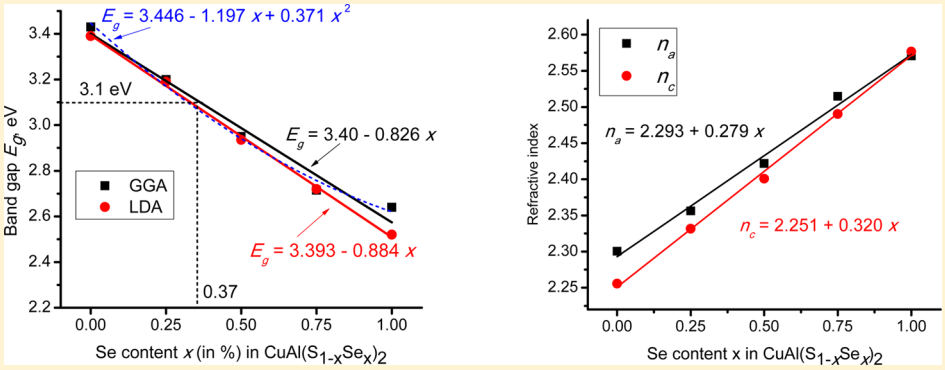

ABSTRACT: Detailed first-principles calculations of the structural, electronic, and optical properties of solid solutions of the promising solar cell material $CuAl(S_{1-x}Se_x)_2$ over the whole range of Se concentration from $x = 0$ to $x = 1$ were performed. It was established that the calculated lattice parameters, band gap, and anisotropic refractive indices vary linearly with the Se concentration. The obtained linear dependences allow for reliable estimations of all these quantities for any value of x, which determines the solid solution composition. The calculated results were compared with the experimental data available for $x = 0$, 0.5, and 1.0; very good agreement was demonstrated, which gives confidence in the properties calculated for other Se concentrations ($x = 0.25, 0.75$). The findings from the present paper can be used in a straightforward way for the successful production of $CuAl(S_{1-x}Se_x)_2$ mixed compounds with desired optoelectronic parameters, which are defined by the composition-tuned mobility of the charge carriers in the upper valence band and the conduction band. Extension of the presented approach to other materials is also possible.

1. INTRODUCTION

Conversion of the energy of the sun into electricity by using solar cells offers a unique opportunity for the ecologically friendly production of electrical energy. Various materials, both organic and inorganic, have been successfully tested for such photovoltaic applications. As a result, remarkable progress in this field has been achieved,[1−4] and the search for new materials with improved performance is never stopped.

The I−III−VI_2 ternary semiconductors with the chalcopyrite structure (e.g., $CuGaS_2$, $CuInS_2$, etc.)[5,6] have been shown to be very suitable materials for solar panels, since they can be grown as thin films,[7−11] which efficiently increases the surface exposed to sunlight. Moreover, the $Cu(In,Ga)(Se,S)_2$ (CIGS)-based solar elements already challenge the dominance of traditional silicon solar panels.[12] The band structure parameters of these materials are influenced by intrinsic defects that form additional trapping levels within the host's band gap. Such defects can significantly change the optical properties of a material, considerably enhancing its optical absorption, and therefore, they play a principal role in optoelectronic and photovoltaic applications. The complex approach, which includes theoretical analysis based on density functional theory (DFT) methods supported by optical experimental studies of the absorption near the band-gap spectral range,[13] is a very powerful tool for predicting the optotlectronic features of materials used for solar panels.

The presence of copper ions in these compounds is a factor that favors d−p charge transfer;[14] they produce an additional contribution to the optical absorption as was shown earlier.[15] Other favorable features of these compounds are their direct band gaps and high absorption coefficients, which allow for a considerable reduction of the film thickness (down to 1−3 μm) compared with traditional silicon thin films, which have thicknesses of about several hundred micrometers.[16]

Received: December 9, 2013
Published: February 11, 2014

   dx.doi.org/10.1021/ic403030w | *Inorg. Chem.* 2014, 53, 2645−2651

To date, ab initio calculations of the properties of chalcopyrite semiconductors have mainly focused on pure compounds from this group,[17−30] and only a limited number of theoretical works related to doped and/or mixed chalcopyrites can be found.

Modification of the composition of these chalcopyrites through doping with various elements (C, Si, Ge, Sn, or d metals) has been suggested.[31,32] Such doping results in the formation of additional energetic states of impurities, which, taken together with the existing intrinsic defect states within the host's band gap, produce additional interband optical transitions that absorb the low-energy photons from the solar spectrum and eventually increase the efficiency of the solar cell materials. Here the main problem is to predict how to vary the cationic−anionic content of such mixed compounds in order to optimize their composition with the aim of achieving the highest absorption efficiency. In this connection, some attention has been paid to the variation of the second cation in chalcopyrite semiconductors. For example, the crystal growth of $CuAl_xGa_{1-x}S_2$ thin films was reported.[33] The presence of Cu ions introduces some nontrivial contribution to the carrier mobilities.[34] In addition, the experimental studies of the spectroscopic properties of $CuGa_xIn_{1-x}S_2$ crystals[35] can be mentioned. Compositional variation may also enhance the electron−phonon anharmonicities,[36] which are extremely strong for this kind of crystal. Those anharmonicities are described by the third-rank polar tensor, and they may form a local electric field capable of influencing and altering the optoelectronic transport properties.

Recently we reported how substitution of the Ga atoms by Al atoms would modify the structural, electronic, optical, and elastic properties of the compounds $CuGa_{1-x}Al_xS_2$ ($x = 0−1$).[37] In particular, it was demonstrated that substitution of 25% of the Ga ions in $CuGaS_2$ by Al ions enhances the absorption properties of $CuGa_{0.75}Al_{0.25}S_2$ in the visible spectral region by about 6% with respect to Al-free $CuGaS_2$. At the same time, the spectral position of the visible absorption band maximum for that mixed $CuGa_{0.75}Al_{0.25}S_2$ compound is still situated very close to the maximum of the solar spectrum. Recently, $CuIn(S_xSe_{1-x})_2$ mixed compounds were studied,[38] and the role played by the partial substitution of selenium by sulfur was considered.

As we have mentioned above, the physical properties of many compounds strongly and quite often unpredictably vary with the changes in the concentration of individual components. Reliable experimental data, if they are known, exist only for some particular compositions of those mixed compounds. In this connection, it is crucial to have a credible method of predicting the properties of composites over the full range of variation of the individual constituents' concentrations. Such methodology not only is important from the point of view of fundamental research, which sheds some light upon the compositional dependence of the materials' physical properties, but also has a high technological significance since it sets the direction for the synthesis of new compounds with desired characteristics. Solar cell materials in this sense occupy a very special place because of the constantly growing demand for their applications.

In the present work, we considered how the variation of the anion composition affects the structural, electronic, and optical properties of $CuAl(S_{1-x}Se_x)_2$ over the whole range of Se concentration from $x = 0$ to $x = 1$. The DFT-based computational approach was used throughout the whole study.

It is obvious that a partial or a complete change of the anion in this case does not alter the crystal structure (except for a rescaling of the lattice parameters). However, the electronic and optical properties defined by the interband energy separations and the band dispersion in **k** space for these mixed compounds are strongly composition-dependent, as will be shown below. Particular interest in these $CuAl(S_{1-x}Se_x)_2$ compounds is backed up by their relatively high absorption coefficients (up to 10^5 cm^{-1}) in the visible spectral range and their potential in applications as blue-to-ultraviolet absorbers and emitters[39,40] as well as by the difference in mobilities of the hole and electron carriers.

The structure of the paper is as follows: in section 2 we describe the structure of the considered materials and details of the calculations; the paper continues with descriptions and discussion of the calculated band structure results (section 3) and optical properties (section 4) and is concluded with a short summary (section 5).

2. CRYSTAL STRUCTURE AND DETAILS OF CALCULATIONS

The elementary cell of $CuAlS_2$ is shown in Figure 1. This material (as well as $CuAlSe_2$) crystallizes in the chalcopyrite structure (space group $I\bar{4}2d$) with four formula units per unit cell. Each atom has four nearest neighbors: every metal ion is coordinated by four sulfur (selenium) ions, and every sulfur (selenium) ion has two Cu and two Al nearest neighbors. The crystal structure data are collected in Table 1. The effects of anion substitution on the properties of the $CuAl(S_{1-x}Se_x)_2$ mixed compounds were studied by gradual substitution of sulfur atoms by selenium atoms with $x = 0$, 0.25, 0.5, 0.75, and 1.0, with subsequent optimization of the crystal structure for each concentration considered.

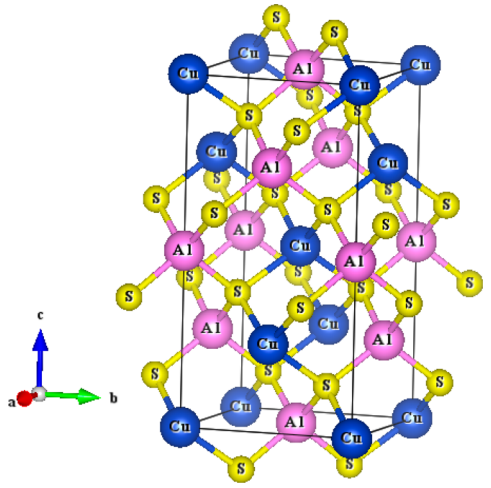

Figure 1. Elementary unit cell of $CuAlS_2$, drawn using the VESTA package.[43]

All of the calculations were performed using the CASTEP module[41] of the Materials Studio package. The exchange−correlation effects were treated within the generalized gradient approximation (GGA) with the Perdew−Burke−Ernzerhof functional.[42] The plane-wave basis set cutoff energy was chosen at 290 eV, and the Monkhorst−Pack scheme **k**-point grid sampling was set as 5 × 5 × 3 **k** points for the Brillouin zone. The convergence tolerance parameters were as follows: energy, 10^{-5} eV/atom; maximal force, 0.03 eV/Å; maximal stress, 0.05 GPa; maximal displacement, 0.001 Å. The calculations were performed for a conventional cell in which eight S atoms were gradually replaced in pairs by Se atoms, corresponding to Se concentrations (in %) of 0, 25, 50, 75, and 100. The considered electronic configurations were

dx.doi.org/10.1021/ic403030w | Inorg. Chem. 2014, 53, 2645−2651

Table 1. Summary of the Experimental and Theoretical Structural Data for the $CuAl(S_{1-x}Se_x)_2$ Compounds

	experiment		calculated, this work: GGA		calculated, this work: LDA		other calculated	
x	a	c	a	c	a	c	a	c
0	5.3336[a]	10.4440[a]	5.28677	10.42678	5.18991	10.37012	5.341,[d] 5.321,[e] 5.2389[f]	10.57,[d] 10.525,[e] 10.4148[f]
0.25			5.36553	10.56518	5.26262	10.5068		
0.5	5.46[b]	10.67[b]	5.44489	10.71706	5.33788	10.62723		
0.75			5.52781	10.83975	5.40848	10.78198		
1	5.606[c]	10.90[c]	5.55587	11.02911	5.48283	10.92691	5.645,[e] 5.53942,[g] 5.47[h]	11.125,[e] 10.9488,[g] 10.90[h]

[a]Reference 44. [b]Reference 45. [c]Reference 46. [d]Reference 47. [e]Reference 48. [f]Reference 49. [g]Reference 50. [h]Reference 51.

$3d^{10}4s^1$ for Cu, $3s^23p^1$ for Al, $3s^23p^4$ for S, and $4s^24p^4$ for Se. All of the obtained results are described and discussed in the next sections.

3. RESULTS OF CALCULATIONS: STRUCTURAL AND ELECTRONIC PROPERTIES

The calculated values of the lattice constants of $CuAl(S_{1-x}Se_x)_2$ in comparison with the experimental results and the results of other calculations (when available) are collected in Table 1. As can be seen, good agreement of our calculated results with the experimental data and the results of other theoretical calculations of the structural properties of pure $CuAlS_2$ and $CuAlSe_2$ was achieved. No experimental and/or theoretical data on the lattice parameters of the mixed compounds $CuAl(S_{1-x}Se_x)_2$ have been reported to date (except for the $x = 0.5$), so the calculated values for $x = 0.25$ and 0.75 reported in Table 1 represent the first theoretical estimations of the lattice constants for these materials.

A good and reliable test for the reasonability of the lattice parameters of those mixed compounds comes from Figure 2,

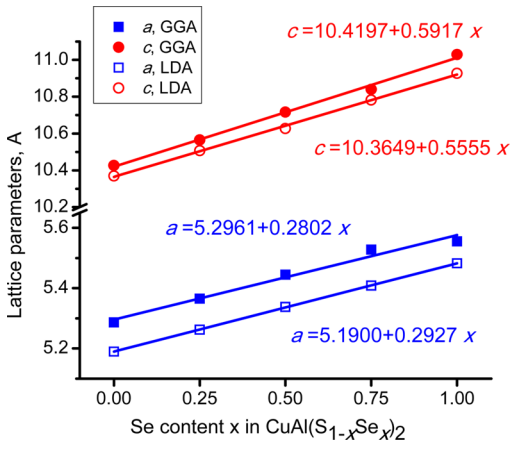

Figure 2. Calculated lattice parameters a and c (solid and open symbols for the GGA and LDA calculations, respectively) and their linear fits (straight lines) as functions of the Se content x in $CuAl(S_{1-x}Se_x)_2$.

which shows the variations of a and c with the Se concentration x. Both of the calculated lattice parameters excellently follow linear trends, which can be anticipated from Vegard's law. The equations of the linear fits given in Figure 2 allow the estimation of the lattice constants of a $CuAl(S_{1-x}Se_x)_2$ alloy for any intermediate value of x varying within the range 0−1. It can be seen that the c constant varies faster with the Se concentration.

Figure 3 shows the calculated band structures of the two pure compounds. The calculated band gap values were 1.93/1.89 eV (GGA/LDA) for $CuAlS_2$ and 1.14/1.02 eV (GGA/LDA) for $CuAlSe_2$. Both values are underestimated compared with the experimental data, which are 3.50 eV for $CuAlS_2$[52] and 2.67 eV for $CuAlSe_2$.[53] At the same time, the calculated results are close to those reported earlier.[47−51] A standard way to overcome such underestimation, which is an intrinsic feature of DFT-based methods, is to introduce the scissor operator, which shifts the conduction band upward until the band gap matches the experimental result. In our case, such an operator was chosen to be 1.5 eV for both neat compounds and was kept at the same value for all of the intermediate compositions. The band structures in Figure 3 are plotted with this scissor value. Figure 3 shows that both the $CuAlS_2$ and $CuAlSe_2$ chalcopyrites possess a direct band gap, with the maximum of the valence band and the minimum of the conduction band realized at the center of the Brillouin zone.

Another principal result that can be deduced from Figure 3 is that there is a considerable difference in the band dispersion for the valence and conduction bands. For the Se-possessing crystals, this difference seems to be substantially larger. It is particularly obvious for the R−X−Γ direction of the Brillouin zone, which may be related to the lower effective masses of the charge carriers in $CuAlSe_2$ with respect to $CuAlS_2$. Although the general shape of the calculated bands may seem to be somewhat similar for the two compounds, one may expect some important differences in the electronic structures in the vicinity of the Γ point, where the conduction band is substantially lower for $CuAlSe_2$ with respect to $CuAlS_2$. This may be a consequence of the larger polarizability of the Se atoms and may be important for the interaction of the trapping levels in the host's band gap with the conduction band states.

It can be noticed from the band structure that there is an energy gap in the valence band between −2 and −3 eV. Its origin can be understood by analyzing the corresponding density of states (DOS) diagrams shown in Figure 4. The upper part of the valence band (between −2 and 0 eV) in all of the considered compounds originates from the Cu 3d states, whereas the 3p (4p) states of S (Se) form the lower part of the valence band from about −3 eV down to −7 eV. The conduction band is mainly due to the Al 3p and 3s states, and the lowest calculated states—the 3s states of S (or 4s states of Se)—are located between −13 and −14.5 eV. There may be d−p charge transfer between the completely filled 3d states of Cu and the completely filled 3p (4p) states of S (Se) due to the d−p hybridization between these orbitals; this is expected to be very important for the formation of the optical properties of the studied compounds.

dx.doi.org/10.1021/ic403030w | Inorg. Chem. 2014, 53, 2645−2651

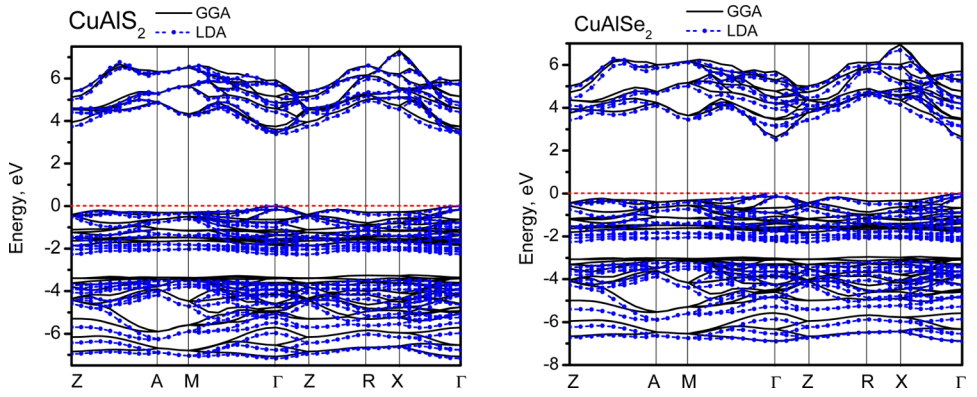

Figure 3. Calculated band structures of $CuAlS_2$ and $CuAlSe_2$. See text for more details. The coordinates of the special points of the Brillouin zone (in units of the reciprocal lattice vectors) are as follows: Z (0, 0, $^1/_2$); A ($^1/_2$, $^1/_2$, $^1/_2$); M ($^1/_2$, $^1/_2$, 0); Γ (0, 0, 0); R (0, $^1/_2$, $^1/_2$); X (0, $^1/_2$, 0).

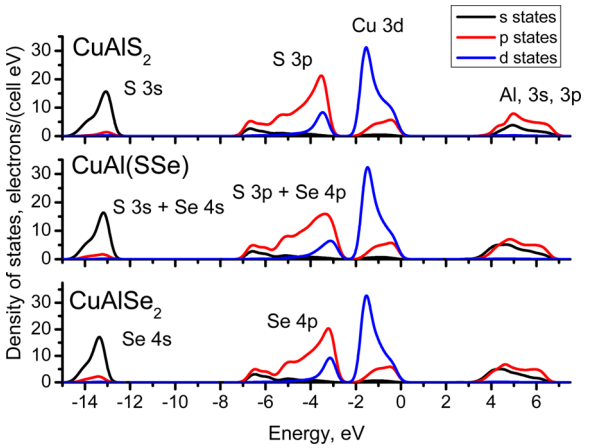

Figure 4. Calculated density of states diagrams for $CuAlS_2$, CuAl(SSe), and $CuAlSe_2$.

4. RESULTS OF CALCULATIONS: OPTICAL PROPERTIES

Figure 5 below shows how the calculated band gap energy for the $CuAl(S_{1-x}Se_x)_2$ compounds varies with composition (the 1.5 eV scissor has been taken into account in this plot). The band gap decreases linearly with increasing Se concentration. The variation of the band gap is practically linear for the LDA calculations; however, in the case of the GGA data (solid squares in Figure 5) a quadratic fit turns out to be somewhat better in describing the energy gap bowing. The functional dependence of the band gap on the selenium concentration provides an opportunity for effective band gap engineering by varying amount of Se in the $CuAl(S_{1-x}Se_x)_2$ solid solution. In particular, it can be noted that at $x \approx 37\%$ the $CuAl(S_{0.63}Se_{0.37})_2$ compound starts to absorb in the visible part of the electromagnetic spectrum at an energy of 3.1 eV. It is also worthwhile to point out that the band gap value of ~3 eV at x = 0.5 with a 1.5 eV scissor operator is in excellent agreement with the experimental band gap value (2.96 eV),[45] which also indicates that the 1.5 eV scissor adequately describes the electronic properties of $CuAl(S_{1-x}Se_x)_2$ compounds over the whole range of concentration x.

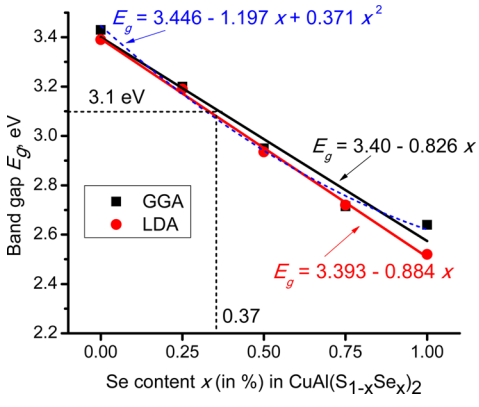

Figure 5. Calculated band gaps of the $CuAl(S_{1-x}Se_x)_2$ compounds (symbols) and their linear (solid lines) and quadratic (dashed line) fits. The equations of the fits are also given. The Se concentration (0.37) corresponding to the threshold of visible range absorption (3.1 eV) is shown.

Figure 6 shows the polarized dielectric function ε as a function of the composition of $CuAl(S_{1-x}Se_x)_2$ (only the GGA results are shown for the sake of brevity). It should be emphasized that these curves were obtained just as a direct result of the performed calculations without any scissor correction. The reason for this is that in this case, the experimental values of the refractive indices of the neat compounds were reproduced best of all without any scissor correction.

In principle, the scissor operator does not modify the wave functions of the initial and final states connected by a dipole transition but only introduces a scaling prefactor before the matrix element of the dipole operator when the transition probability is calculated. However, as was mentioned above, such a correction, although required to make the calculated band gap match the experimental results, did not turn out to be needed for the calculations of the optical properties described below.

The ε_a, ε_b, and ε_c notations correspond to the (1, 0, 0), (0, 1, 0) and (0, 0, 1) polarizations. The shapes of the curves are substantially asymmetrical. This may favor an interaction with the phonon subsystem. It can be also seen that the value of Re(ε) increases with decreasing band gap E_g (i.e., with increasing Se concentration). Such an observation is in line with the Penn model,[54] in the framework of which $\varepsilon(0) \approx 1 + (\hbar\omega_p/E_g)^2$, where $\hbar\omega_p$ stands for the plasma energy.

As evidenced by the calculated curves, there is a noticeable anisotropy of the optical constant dispersion. This is even more pronounced when the values of the refractive indices n_a and n_c are shown (Figure 7). These values can be obtained by taking a square-root extrapolation of the corresponding Re(ε) to zero

dx.doi.org/10.1021/ic403030w | Inorg. Chem. 2014, 53, 2645−2651

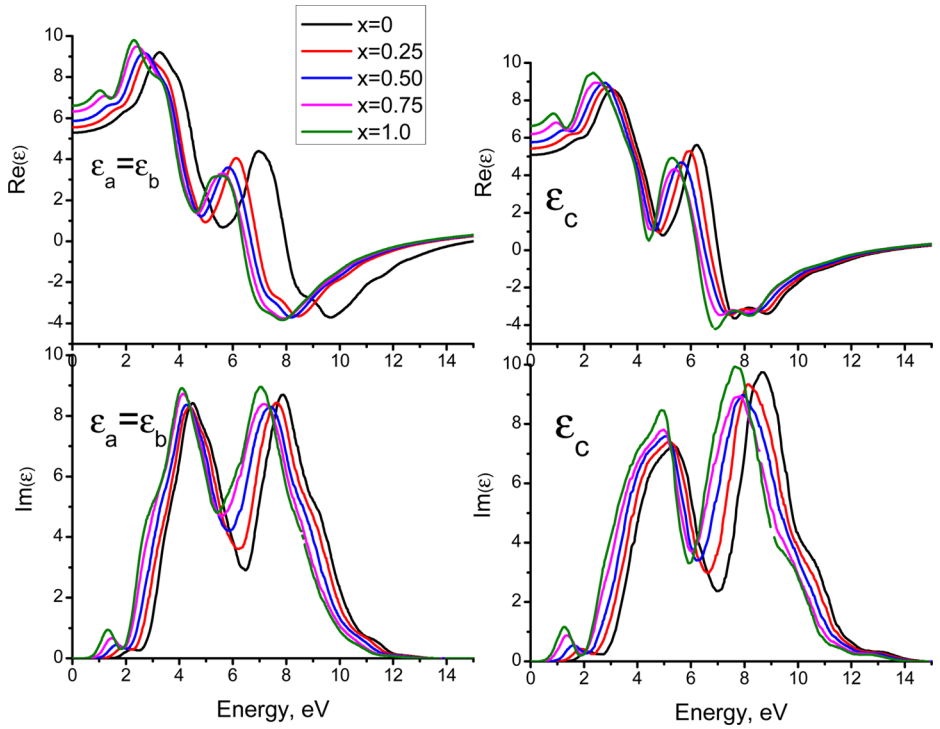

Figure 6. Calculated polarized real part, Re(ε), and imaginary part, Im(ε), of the dielectric function ε for the $CuAl(S_{1-x}Se_x)_2$ compounds.

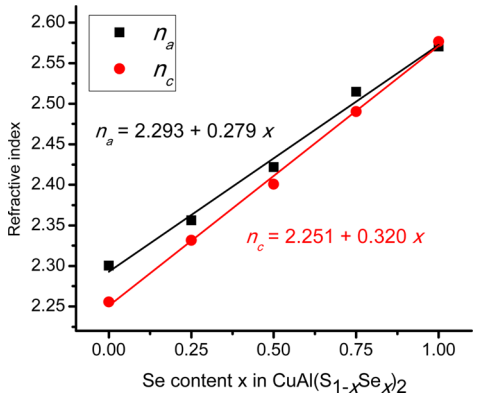

Figure 7. Calculated polarized refractive indices for the $CuAl(S_{1-x}Se_x)_2$ compounds.

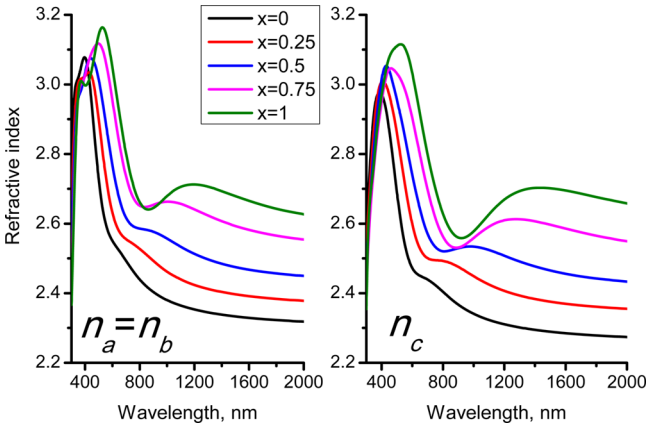

Figure 8. Calculated dispersions of the refractive indices for the $CuAl(S_{1-x}Se_x)_2$ compounds.

energy (infinite wavelength). The calculated values of the refractive indices of $CuAlS_2$ turned out to be n_a = 2.30 and n_c = 2.25, which are very close to the experimental value of 2.378.[55] As far as the refractive index of $CuAlSe_2$ is concerned, its experimental value is about 2.492[55] or 2.600,[56] which also is close to our calculated result of 2.57 (Figure 7). Therefore, having obtained good agreement between the calculated and experimental values of the refractive index for $CuAlS_2$ and $CuAlSe_2$, we calculated these values also for intermediate values of x, as shown in Figure 7. Again, both n_a and n_c are almost perfect linear functions of the Se concentration. The linear fits and the resulting linear functions of the Se concentration obtained for both n_a and n_c allow for estimation of the refractive index of the $CuAl(S_{1-x}Se_x)_2$ solid solution for any anion composition.

Figure 8 shows the dispersions of the calculated refractive indices in the spectral region between 350 and 2000 nm. The range of variation of the refractive index is relatively wide, from about 2.25 in the long-wavelength limit to 3.15−3.17 at about 500 nm.

Finally, in Figure 9 we show the birefringence, $\Delta n = n_c - n_a$,[57] for all of the studied compounds. The birefringence changes sign from positive to negative in moving from neat $CuAlS_2$ to neat $CuAlSe_2$. Its absolute value is also increasing in the spectral range close to the band gap, and this maximum moves toward longer wavelength with increasing Se content since the band gap decreases in that case.

5. CONCLUSIONS

In the present work, we have considered how the gradual substitution of S by Se in the $CuAlS_2$ chalcopyrite semiconductor affects its structural, electronic, and optical properties. By means of first-principles calculations (using the CASTEP module of Materials Studio), we have shown that the calculated lattice parameters, band gaps, and anisotropic

dx.doi.org/10.1021/ic403030w | Inorg. Chem. 2014, 53, 2645−2651

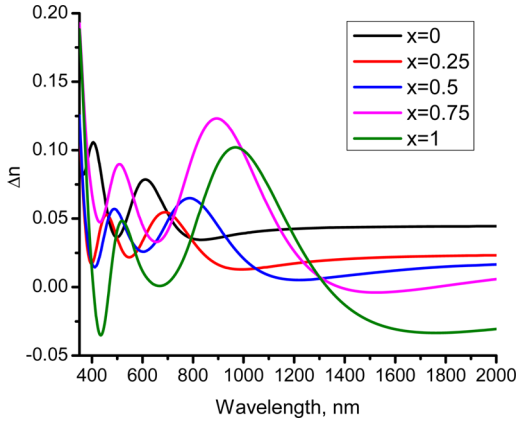

Figure 9. Calculated birefringence for the $CuAl(S_{1-x}Se_x)_2$ compounds.

refractive indices of the mixed $CuAl(S_{1-x}Se_x)_2$ solid solutions all are linear functions of the Se concentration x over the whole range of concentrations from 0 to 1. The obtained results are in very good agreement with the experimental data, which are available for x = 0, 0.5, and 1.0.

The neat $CuAlS_2$ and $CuAlSe_2$ chalcopyrites as well as the $CuAl(S_{1-x}Se_x)_2$ mixed compounds possess a direct band gap, with the maximum of the valence band and the minimum of the conduction band occurring at the center of the Brillouin zone. The encountered difference in the dispersions of the electronic states suggests a lower effective mass of the charge carriers in $CuAlSe_2$ in comparison with $CuAlS_2$.

The obtained functional dependences of the calculated properties of $CuAl(S_{1-x}Se_x)_2$ allow for their meaningful and reliable estimation for any anion composition. Therefore, the obtained results are important for smart materials engineering, as they provide the opportunity to find the particular Se concentration x that would lead to the desired properties (lattice parameters, band gap, index of refraction) of a $CuAl(S_{1-x}Se_x)_2$ solid solution.

AUTHOR INFORMATION

Corresponding Author

*E-mail: brik@fi.tartu.ee. Phone: +372 7374751.

Notes

The authors declare no competing financial interest.

ACKNOWLEDGMENTS

M.G.B. appreciates the financial support from (i) the European Social Fund's Doctoral Studies and Internationalisation Programme DoRa, (ii) the European Union through the European Regional Development Fund (Center of Excellence "Mesosystems: Theory and Applications", TK114), (iii) the Marie Curie Initial Training Network LUMINET (Grant Agreement 316906), (iv) Jan Dlugosz University during his visiting professorship in November−December 2013, and (v) the Programme for the Foreign Experts offered by Chongqing University of Posts and Telecommunications. For this work, M.P. and I.K. were supported by the Polish National Science Centre (under Project 2011/01/B/ST7/06194). Dr. G. A. Kumar (University of Texas at San Antonio) is thanked for allowing us to use the Materials Studio package.

REFERENCES

(1) Guenes, S.; Neugebauer, H.; Sariciftci, N. S. *Chem. Rev.* **2007**, *107*, 1324.
(2) Hoppe, H.; Sariciftci, N. S. *J. Mater. Res.* **2004**, *19*, 1924.
(3) Grätzel, M. *Acc. Chem. Res.* **2009**, *42*, 1788.
(4) Contreras, M. A.; Egaas, B.; Ramanathan, K.; Hiltner, J.; Swartzlander, A.; Hasoon, F.; Noufi, R. *Prog. Photovoltaics* **1999**, *7*, 311.
(5) Romanyuk, Y. E.; Marushko, L. P.; Piskach, L. V.; Kityk, I. V.; Fedorchuk, A. O.; Pekhnyo, V. I.; Parasyuk, O. V. *CrystEngComm* **2013**, *15*, 4838.
(6) Gorgut, G. P.; Fedorchuk, A. O.; Kityk, I. V.; Sachanyuk, V. P.; Olekseyuk, I. D.; Parasyuk, O. V. *J. Cryst. Growth* **2011**, *324*, 212.
(7) Jeong, W.-J.; Park, G.-C. *Sol. Energy Mater. Sol. Cells* **2003**, *75*, 93.
(8) Martí, A.; Marrón, D. F.; Luque, A. *J. Appl. Phys.* **2008**, *103*, No. 073706.
(9) Marsen, B.; Klemz, S.; Unold, T.; Schock, H.-W. *Prog. Photovoltaics* **2011**, *20*, 625.
(10) Jager-Waldau, A. *Sol. Energy Mater. Sol. Cells* **2011**, *95*, 1509.
(11) Yamaguchi, T.; Asai, Y.; Oku, N.; Niiyama, S.; Imanishi, T.; Nakamura, S. *Sol. Energy Mater. Sol. Cells* **2011**, *95*, 274.
(12) Repins, I.; Contreras, M. A.; Egaas, B.; DeHart, C.; Scharf, J.; Perkins, C. L.; To, B.; Noufi, R. *Prog. Photovoltaics* **2008**, *16*, 235.
(13) Brik, M. G.; Kityk, I. V.; Parasyuk, O. V.; Myronchuk, G. L. *J. Phys.: Condens. Matter* **2013**, *25*, No. 505802.
(14) Baidakov, D. L. *Russ. J. Appl. Chem.* **2013**, *86*, 1351.
(15) Al-Harbi, E.; Wojciechowski, A.; AlZayed, N.; Parasyuk, O. V.; Gondek, E.; Armatys, P.; El-Naggar, A. M.; Kityk, I. V.; Karasinski, P. *Spectrochim. Acta, Part A* **2013**, *111*, 142.
(16) Saji, V. S.; Lee, S. M.; Lee, C. W. *J. Korean Electrochem. Soc.* **2011**, *14*, 61.
(17) Lany, S.; Zunger, A. *Phys. Rev. B* **2005**, *72*, No. 035215.
(18) Vidal, J.; Botti, S.; Olsson, P.; Guillemoles, J.-F.; Reining, L. *Phys. Rev. Lett.* **2010**, *104*, No. 056401.
(19) Chen, S.; Gong, X. G.; Wei, S.-H. *Phys. Rev. B* **2007**, *75*, No. 205209.
(20) Maeda, T.; Takeichi, T.; Wada, T. *Phys. Status Solidi A* **2006**, *203*, 2634.
(21) Rodriguez, J. A.; Quiroga, L.; Camacho, A.; Baquero, R. *Phys. Rev. B* **1999**, *59*, 1555.
(22) Ahuja, R.; Auluck, S.; Eriksson, O.; Wills, J. M.; Johansson, B. *Sol. Energy Mater. Sol. Cells* **1998**, *53*, 357.
(23) Choi, I.-H.; Han, S.-D.; Eom, S.-H.; Lee, W.-H.; Lee, H. C. *J. Korean Phys. Soc.* **1996**, *29*, 377.
(24) Syrbu, N. N.; Bogdanash, M.; Tezlevan, V. E.; Stamov, I. G. *J. Phys.: Condens. Matter* **1997**, *9*, 1217.
(25) Laksari, S.; Chahed, A.; Abbouni, N.; Benhelal, O.; Abbar, B. *Comput. Mater. Sci.* **2006**, *38*, 223.
(26) Brik, M. G. *J. Phys.: Condens. Matter* **2009**, *21*, No. 485502.
(27) Soni, A.; Gupta, A.; Arora, C. M.; Dashora, A.; Ahuja, B. L. *Sol. Energy* **2010**, *84*, 1481.
(28) Aguilera, I.; Vidal, J.; Wahnón, P.; Reining, L.; Botti, S. *Phys. Rev. B* **2011**, *84*, No. 085145.
(29) Romero, A. H.; Cardona, M.; Kremer, R. K.; Lauck, R.; Siegle, G.; Hoch, C.; Munoz, A. *Phys. Rev. B* **2011**, *83*, No. 195208.
(30) Soni, A.; Dashora, A.; Gupta, V.; Arora, C. M.; Ahuja, B. L. *Int. J. Sustainable Energy* **2013**, *32*, 18.
(31) Tablero, C. *Thin Solid Films* **2010**, *519*, 1435.
(32) Tablero, C.; Marrón, D. F. *J. Phys. Chem. C* **2010**, *114*, 2756.
(33) Harada, Y.; Nakanishi, H.; Chichibu, S. F. *J. Cryst. Growth* **2001**, *226*, 473.
(34) Kavetskyy, T. S.; Valeev, V. F.; Nuzhdin, V. I.; Tsmots, V. M.; Stepanov, A. L. *Tech. Phys. Lett.* **2013**, *39*, 1.
(35) Syrbu, N. N.; Tiginyanu, I. M.; Nemerenco, L. L.; Ursaki, V. V.; Tezlevan, V. E.; Zalamai, V. V. *J. Phys. Chem. Solids* **2005**, *66*, 1974.
(36) Han, M. J.; Savrasov, S. Y. *Phys. Rev. Lett.* **2009**, *103*, No. 067001.
(37) Brik, M. G.; Ma, C.-G. *J. Phys. D: Appl. Phys.* **2013**, *46*, No. 285304.
(38) Wan, F. C.; Tang, F. L.; Zhu, Z. X.; Xue, H. T.; Lu, W. J.; Feg, Y. D.; Rui, Z. Y. *Mater. Sci. Semicond. Process.* **2013**, *16*, 1422.

(39) Chichibu, S.; Matsumoto, S.; Shirakata, S.; Isomura, S.; Higuchi, H. *J. Appl. Phys.* **1993**, *74*, 6446.
(40) Shim, Y.; Hasegawa, K.; Wakita, K.; Mamedov, N. *Thin Solid Films* **2008**, *517*, 1442.
(41) Segall, M. D.; Lindan, P. J. D.; Probert, M. J.; Pickard, C. J.; Hasnip, P. J.; Clark, S. J.; Payne, M. C. *J. Phys.: Condens. Matter* **2002**, *14*, 2717.
(42) Perdew, J. P.; Burke, K.; Ernzerhof, M. *Phys. Rev. Lett.* **1996**, *77*, 3865.
(43) Momma, K.; Izumi, F. *J. Appl. Crystallogr.* **2011**, *44*, 1272.
(44) Brandt, G.; Rauber, A.; Schneider, J. *Solid State Commun.* **1973**, *12*, 481.
(45) Ho, C.-H.; Pan, C.-C. *Opt. Express* **2013**, *3*, 480.
(46) Hahn, H.; Frank, G.; Klingler, W.; Meyer, A.-D.; Störger, G. *Z. Anorg. Allg. Chem.* **1953**, *271*, 153.
(47) Verma, U. P.; Jensen, P.; Sharma, M.; Singh, P. *Comput. Theor. Chem.* **2011**, *975*, 122.
(48) Zhou, H. G.; Chen, H.; Chen, D.; Li, Y.; Ding, K. N.; Huang, X.; Zhang, Y. F. *Acta Phys.-Chim. Sin.* **2011**, *27*, 2805.
(49) Parlak, C.; Eryiğit, R. *Phys. Rev. B* **2004**, *70*, No. 075210.
(50) Li, D.; Ling, F. R.; Zhu, Z. Y.; Zhang, H. Y.; Zhang, X. H. *J. Phys. Chem. Solids* **2012**, *73*, 617.
(51) Abdellaoui, A.; Ghaffour, M.; Bouslama, M.; Benalia, S.; Ouerdane, A.; Abidri, B.; Monteil, Y. *J. Alloys Compd.* **2009**, *487*, 206.
(52) Yoodee, K.; Woolley, J. C.; Sa-yakanit, V. *Phys. Rev. B* **1984**, *30*, 5904.
(53) Jaffe, J. E.; Zunger, A. *Phys. Rev. B* **1983**, *28*, 5822.
(54) Penn, D. R. *Phys. Rev.* **1962**, *128*, 2093.
(55) Xue, D.; Betzler, K.; Hesse, H. *Phys. Rev. B* **2000**, *62*, 13546.
(56) Alonso, M. I.; Pascual, J.; Garriga, M.; Kikuno, Y.; Yamamoto, N.; Wakita, K. *J. Appl. Phys.* **2000**, *88*, 1923.
(57) Reshak, A. H. *Physica B* **2005**, *369*, 243.